SUBCOOLED BOILING CRITICAL HEAT FLUX OF WATER FLOWING UPWARD IN A TUBE FOR LOWER FLOW AND PRESSURE UP TO 20 MPa

Y. Chen, C. Yang, M. Zhao, K. Bi, K. Du and S. Zhang

China Institute of Atomic Energy, China Email: chenyz@ciae.ac.cn

Abstract

An experiment of critical heat flux was conducted in an inconel tube of inner diameter of 7.98 mm and heating length of 0.8 m with water flowing upward, covering the ranges of pressure of 1.96 - 20.4 MPa, mass flux of 476 - 1653 kg/m²s, inlet subcooling of 49 - 346 K and exit subcooling of 1 - 158 K. Based on the experimental result, an empiric correlation was formulated and the parametric trends were studied systematically. A physical model was proposed with assumption of critical thickness of bubbly layer.

Keywords: critical heat flux (CHF), near-critical, supercritical water cooled reactor, subcooled boiling

Introduction

The critical heat flux (CHF) is a major limit for the safety of nuclear reactors because the occurrence of critical heat flux could lead to a failure of fuel element. For supercritical water-cooled reactor (SCWR), in startup and shutdown periods or accident conditions, the system will experience subcritical pressure, and the accurate estimation of critical heat flux is a concern.

During past five decades the CHF has been investigated extensively over the world theoretically and experimentally, and a variety of prediction methods have been available, as summarized in a IAEA technical document [1]. In general, great majority of existing studies were related to the conditions of current pressurized water reactor (PWR), while the studies for higher pressures and lower flow rate, which is interest of SCWR, were relatively scarce. So far, the experiments of near-critical pressure were mostly performed with medium of freon [2-4], but few with water [5]. Therefore, the existing prediction methods for CHF are not validated adequately for the SCWR condition

In the author's previous investigation an experiment of critical heat flux in subcooled boiling of water was performed in a stainless-steel tube at near-critical condition, and the CHF characteristics were studied preliminarily [6]. It was observed that the surface deposit could produce a prematurity of CHF. It could not be avoided completely in the loop, though de-ioned water was used. This negative effect appeared more appreciable at higher pressure. In the present experiment an inconel tube was used for the test section, and the test loop was modified by

installing an ion-exchanger upstream of the test section to improve the purity of water. By adopting this measure the effect of surface condition due to the deposit was diminished ultimately, and then the CHF was studied systematically over a wide range of pressure. Based on the experimental data a physical model was proposed.

1. Experimental facility and procedure

The test section is an inconel-625 tube of 7.98 mm in inner diameter and 9.65 mm in outer diameter with water flowing upward inside. It provides uniform heat flux over a length of 0.8 m. There is a leading un-heating length of 0.6 m for full development of hydraulic condition.

The experiment was performed at a supercritical water loop in China Institute of Atomic Energy (CIAE). To improve the purity of water ultimately, in the present experiment an ion-exchanger was installed upstream of the preheater. The schematic diagram of the loop is shown in Fig. 1.

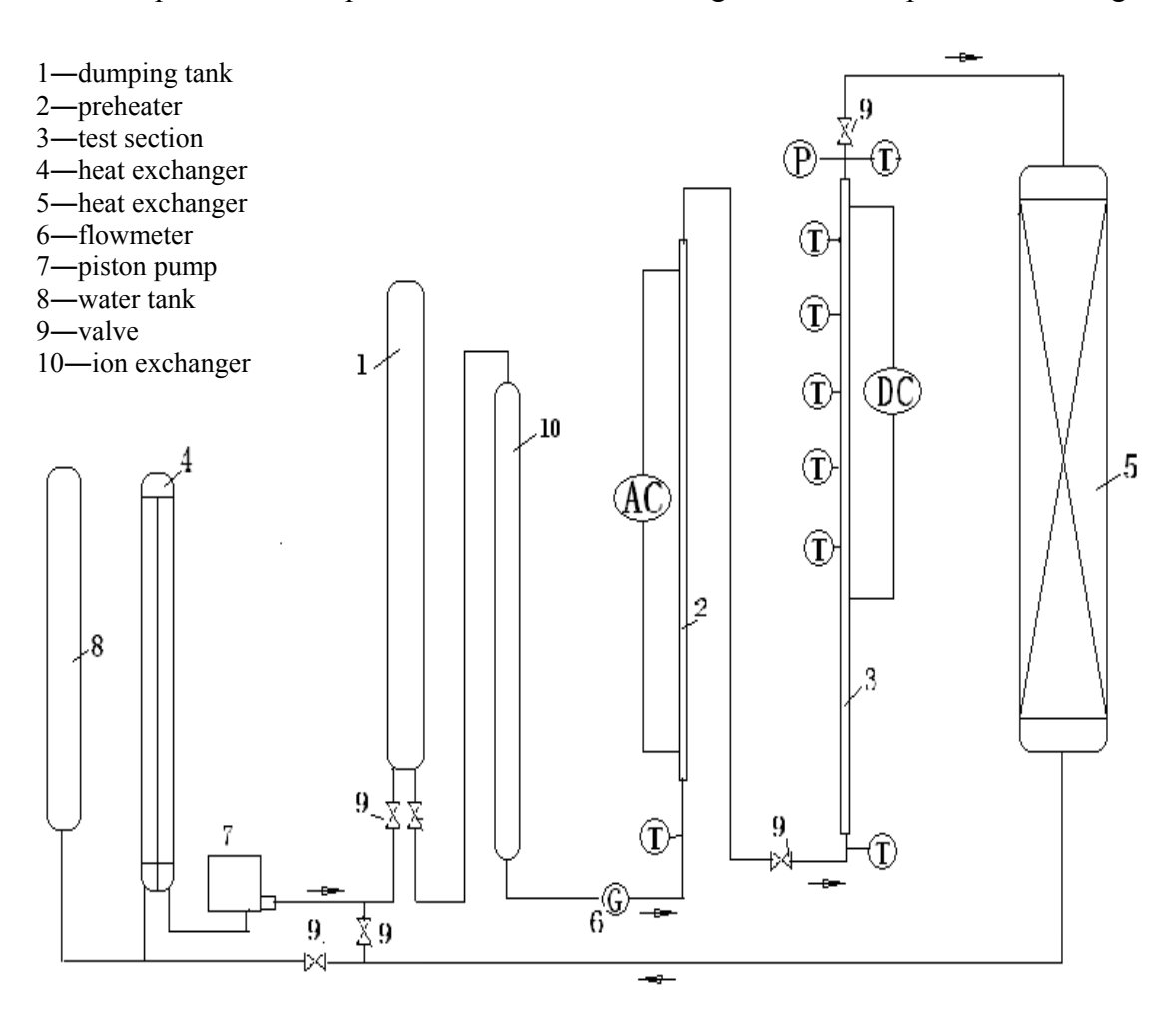


Figure 1 Schematic diagram of the test loop

The de-ioned water was supplied by a three-head piston pump with a maximum pressure of 45 MPa and a flow rate of 2.4 m³/h. It passed a dumping tank, the ion-exchanger and a preheater, sequentially, and flowed upward through the test section,. Then it was cooled by heat exchangers, and finally flowed back to the pump. The flow rate of the test section was controlled by valves in bypass and main path, and the inlet temperature was controlled by the power to preheater. The test section was heated by a DC supply with capacity of 7,000 A×65 V, and the preheater was heated by an AC supply. With this system the experiment can be performed at stable conditions.

Major measurements of the parameters included: the outlet pressure by a pressure transducer (DCY-1151), the flow rate by a turbine flow-meter (LWGY-6), the inlet and outlet water temperatures of the test section by NiCr-NiSi thermocouples and the voltage and current across the test section. All the readings were recorded by a data acquisition system. The occurrence of boiling crisis was detected by photocells.

During test, at first a desired pressure, flow rate and inlet temperature were established. Then, the power to test section was switched on. The boiling crisis was approached by increasing the power to test section step by step, keeping the pressure, the flow rate and the inlet temperature at constant. When the condition was close to the CHF the increase of power for each step was less than 0.3%, until the occurrence of boiling crisis was detected by photocell, which switched off the power to the test section. The heat balances of all the runs were within 3.5% with majority within 2%.

2. Experimental results

Totally 193 data of critical heat flux were obtained, covering the ranges of pressure of p = 1.96 - 20.4 MPa, mass flux of G = 476 - 1653 kg/m²s, inlet subcooling of $DT_{s,i} = 49 - 346$ K, outlet subcooling of $DT_{s,o} = 1 - 158$ K and critical heat flux of $q_{CHF} = 0.26 - 4.95$ MW/m².

For low mass flux the CHF is closely related to the inlet condition, characterizing the mechanism of total power dominant. This behavior was also observed in the previous experiment. To consider this characteristic the present experimental data are formulated as the following empiric correlation,

$$q_{CHF} = cq_s \tag{1}$$

where q_s is the heat flux for the exit to reach saturation temperature, as

$$q_s = \frac{(H_s - H_i)GD}{4l}$$

$$c = Min \left[2350(1 - 0.0307 p)(G(H_s - H_i))^{-0.35}, 1.0 \right]$$
(2)

and

where p is the pressure, H_i and H_s the inlet enthalpy and saturation enthalpy, respectively, G the mass flux, D the diameter and l the heating length.

In Fig.2 the experimental results are compared with the predictions of Eq.(1) by displaying the ratio of calculated to measured CHF, $R = q_{CHF,C} / q_{CHF,M}$, versus p, G, $DT_{s,i}$ and $DT_{s,o}$, respectively. The average deviation, AVG, is 0.75% and the standard deviation, RMS, is 5.34%.

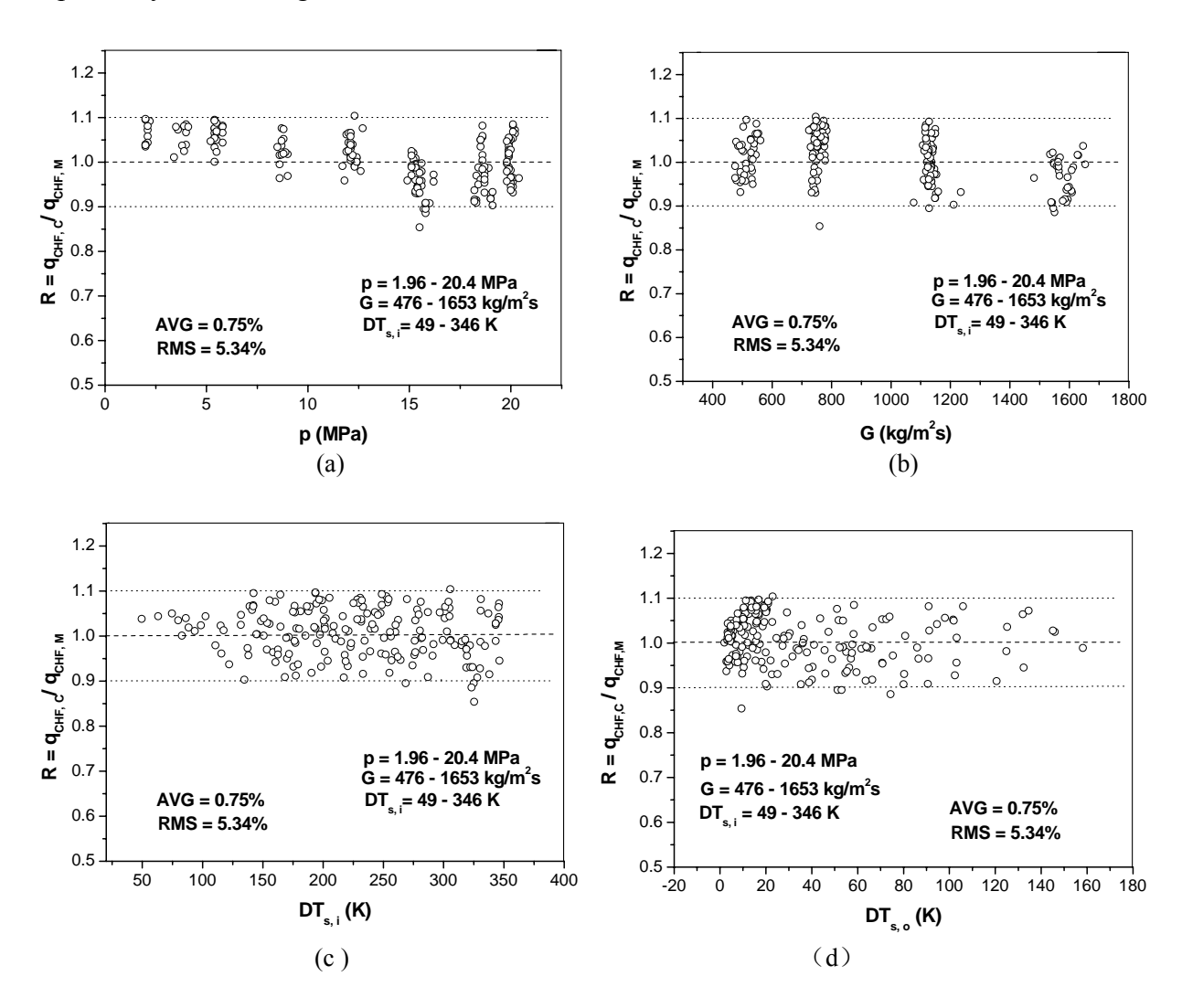


Figure 2 Calculations of experimental results by Eq.(1)

2.1 Parametric trends

The experimental results are shown in Fig.3 and 4 by $q_{CHF} \sim DT_{s,i}$ for different mass fluxes and different pressures, respectively. As seen, the critical heat flux increases monotonously as the inlet subcooling increasing, and higher mass flux corresponds to higher critical heat flux. It is observed in the results that in low $DT_{s,o}$ region a small variation of $DT_{s,o}$ might correspond to larger difference in $DT_{s,i}$, associated with greater difference in CHF, as exemplified in Fig.5 by $q_{CHF} \sim DT_{s,o}$. This behavior suggests the effect of inlet condition on CHF and the mechanism of total power dominant under this condition.

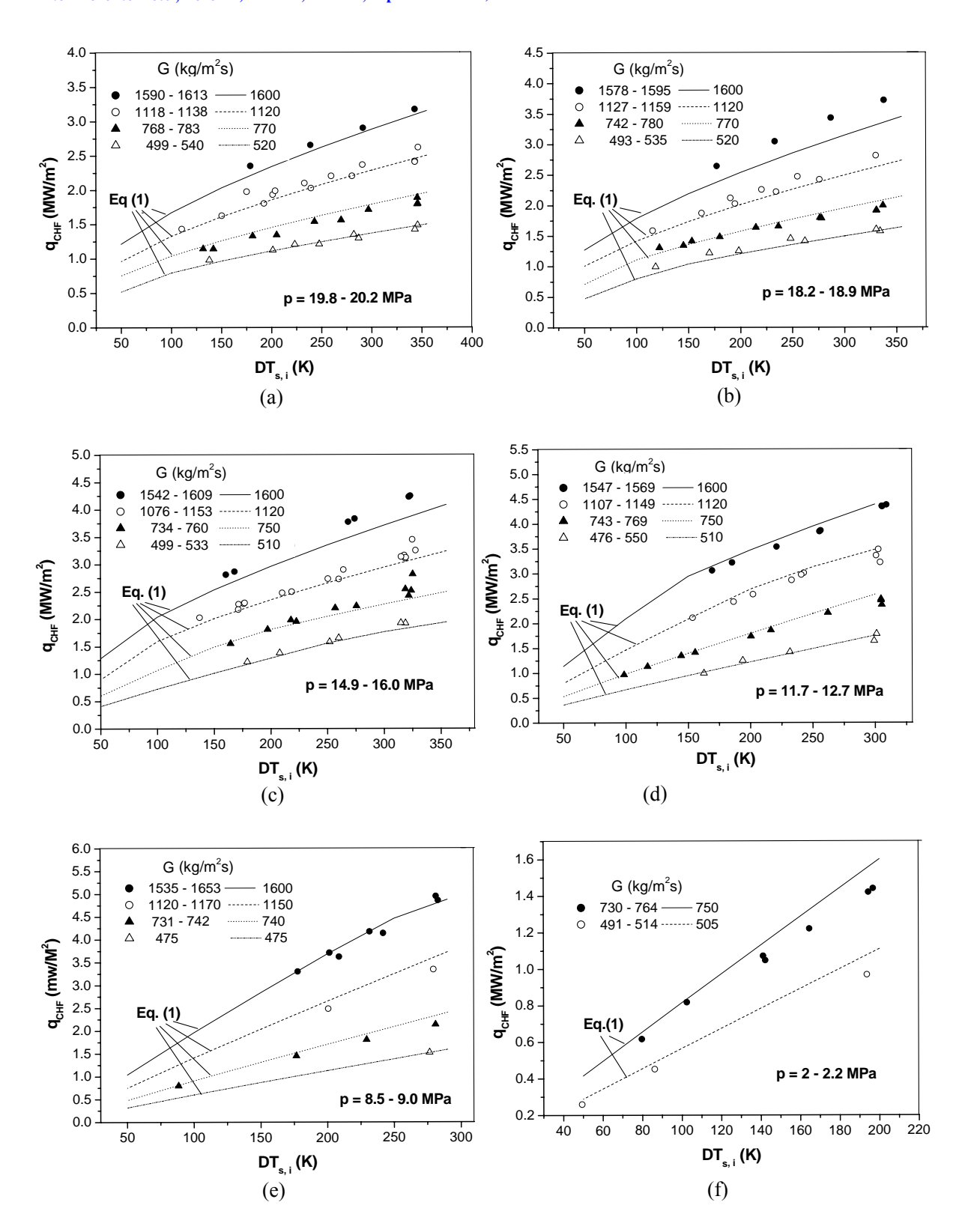


Figure 3 Variations of CHF with DT_{s, i} for different mass fluxes

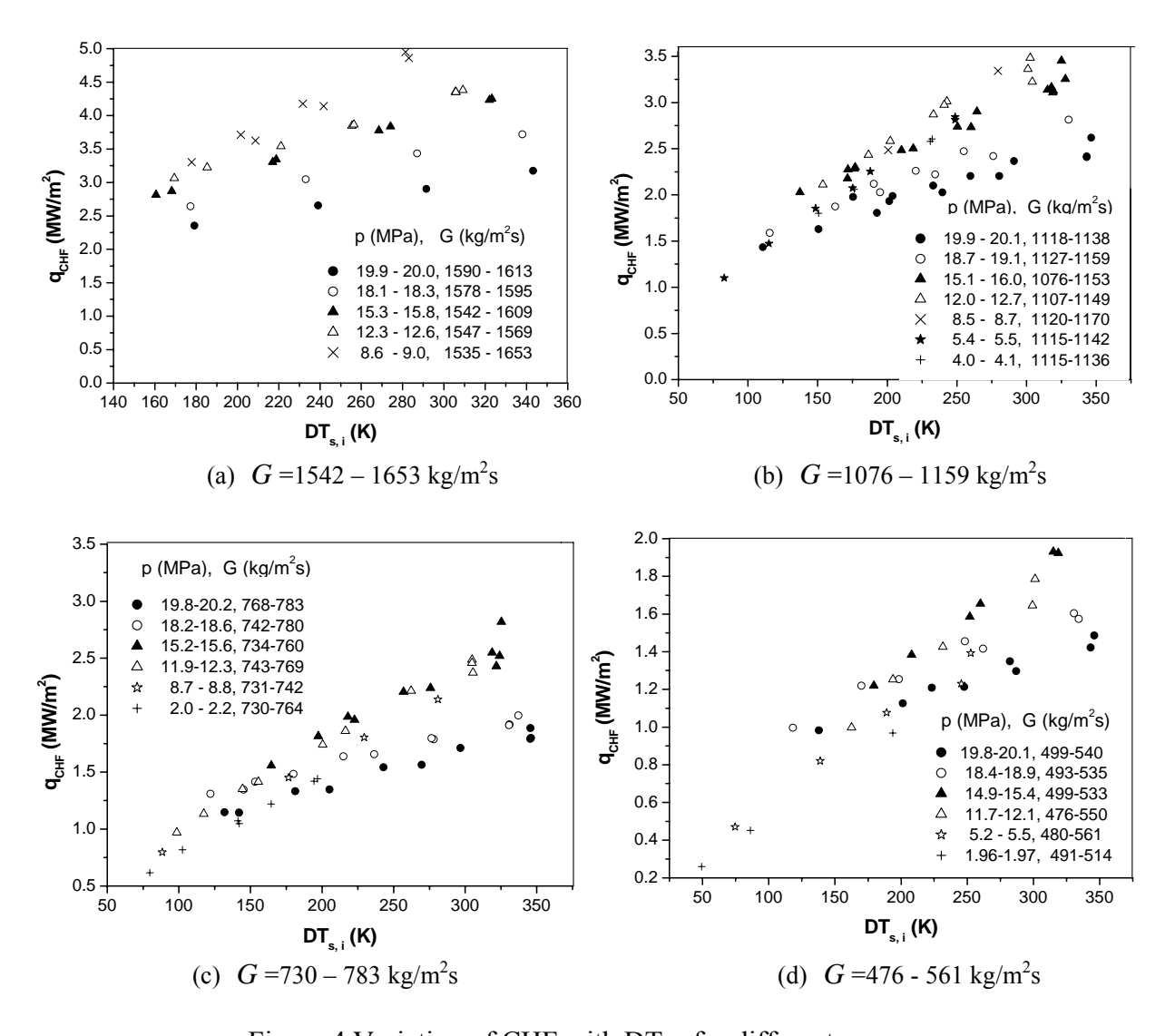


Figure 4 Variation of CHF with DT_{s, i} for different pressures

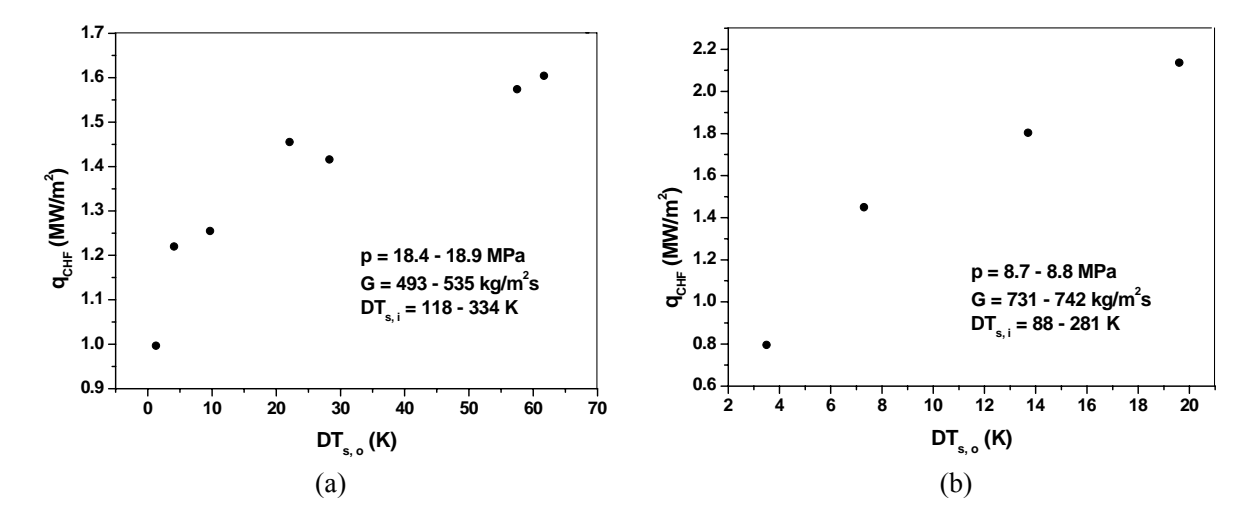


Figure 5 Variations of CHF with DT_{s, o}

For lower pressure the effects of inlet subcooling and mass flux appear stronger than higher pressure, associated with complicated effect of pressure on CHF. For $G > 1500 \text{ kg/m}^2\text{s}$ the CHF of p > 18 MPa are much lower than lower pressure, especially in high subcooling region (Fig.4(a)). For $G = 700 - 1200 \text{ kg/m}^2\text{s}$ with low subcooling the results are not different appreciably between different pressures (Fig.4 (b) and (c)). For $G < 600 \text{ kg/m}^2\text{s}$, in high $DT_{s,i}$ region the results of p > 18 MPa are lower than those of p < 16 MPa, while in low $DT_{s,i}$ region the results show an opposite trend (Fig.4 (d)). The effect of pressure on CHF can also be observed distinctly in Fig.6 by $q_{CHF} \sim p$. In general, as the pressure increases toward the critical point the CHF tends to decrease, and it appears severer as mass flux increases. For $G > 1500 \text{ kg/m}^2\text{s}$ the CHF drops significantly at near-critical pressure.

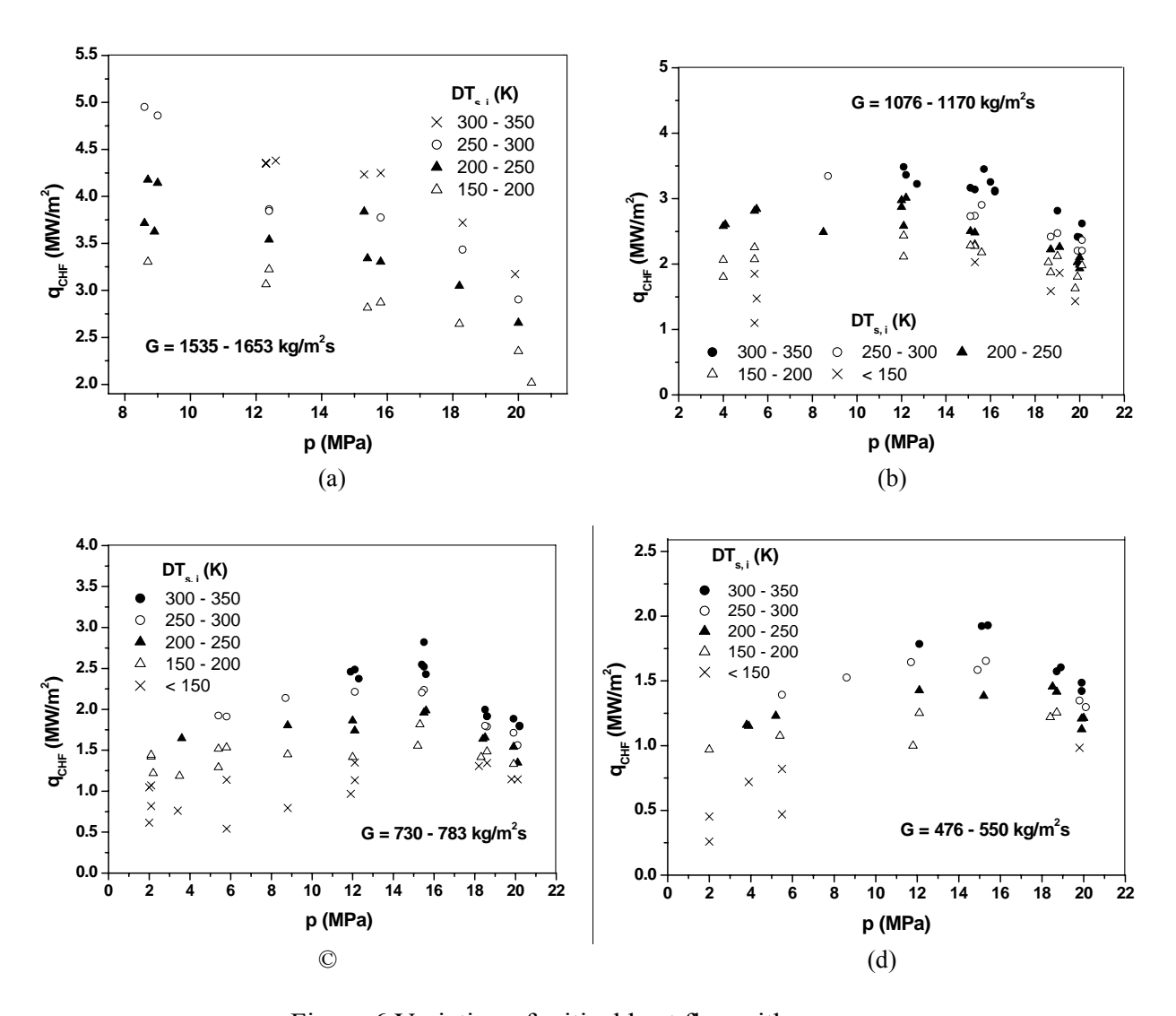


Figure 6 Variation of critical heat flux with pressure

2.2 Effect of material

In the previous experiment the test section was made of a stainless-steel tube with inner diameter of 7.95 mm and heating length of 0.8 m. The deposit on surface was found to have an appreciable effect on the CHF. The surface of test tube was cleaned every two or three runs to diminish this effect essentially, and the CHF data were obtained, covering the ranges of p = 8.6 - 20.9 MPa, mass flux of 447 - 1179 kg/m²s and inlet subcooling of 116 - 347 K. The surface of inconel tube used in the present experiment looks smoother than the stainless-steel tube. The previous data are calculated by Eq.(1), and the ratio of calculated to measured values are shown in Fig.7. As seen, the results of p < 15 MPa are not different appreciably between two experiments, while for p > 18 MPa the data of stainless-steel tube are underpredicted by about 10%.

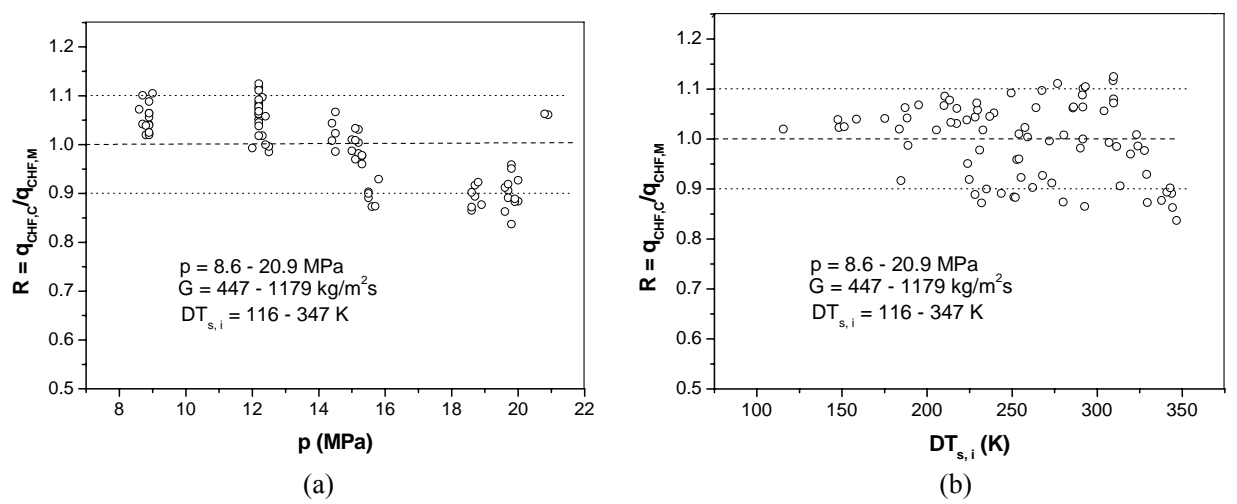


Figure 7 Predictions of the previous experimental results in stainless- steel tube [6] with Eq.(1)

3. Physical Model

In subcooled flow boiling the enthalpy of bubbly layer is determined by the heat transfer from the interface of bubbly layer to liquid core, and the excessive bubble crowding serves as a thermal shield, leading to the onset of CHF. Various CHF models have been available with different assumptions of the mechanisms [7, 8]. The critical enthalpy models were proposed by Weisman and Pei [9] and Tong [10], in which the heat transfer coefficient from the interface of bubbly layer to liquid core was estimated by a simple empiric correlation. The liquid sublayer dryout models were proposed by Katto [11], Lee and Mudawar [12] and Celata et al. [8], in which the sublayer dryout was dominated by the bubble diameter, the thickness of liquid sublayer and the length of vapor blanket.

For subcooling larger than a certain value the major part of heat from wall is transferred to the liquid core to increase the liquid enthalpy, while the heat for increase of the enthalpy of bubbly layer takes only a small percentage of the total heat. Therefore, the characteristic of bubbly layer

is heavily controlled by the heat transfer from the bubbly layer to liquid core. This heat transfer is closely relative to the turbulence near the edge of the bubbly layer, which is sensitive to the distance from the wall. The increase in the thickness of bubbly layer associates with an increase in the heat transfer capability to the liquid core, but also with an increase in the thermal resistance of the bubbly layer. The balance of these two factors gives a critical value of the thickness. Therefore, in the liquid sublayer dryout model the mechanism of CHF is virtually the limiting heat transfer capability from the interface of bubbly layer, and the thickness of bubbly layer is a key parameter.

In Fig.8 the present experimental results are compared with the calculations of Celata's model. The average error, AVG, and standard error, RMS, are -6.0% and 11.2%, respectively. The underprediction by this model is mostly related to low subcooling condition. This could be due to the fact that the Celata model was derived for high flow and high subcooling condition, in

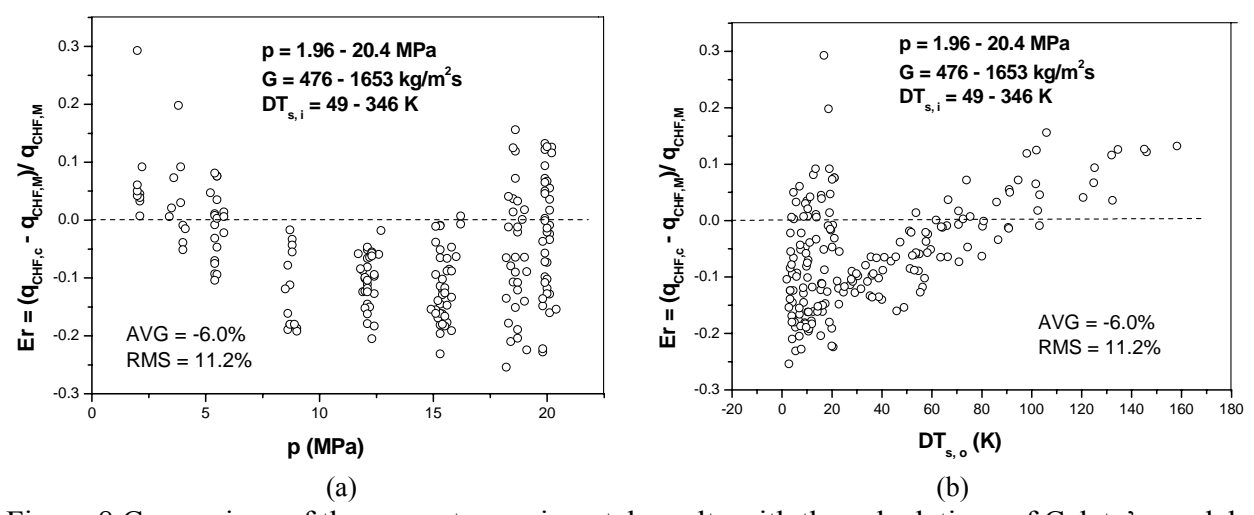


Figure 8 Comparison of the present experimental results with the calculations of Celata's model

which the thickness of bubbly layer was determined by the size of a bubble. This could not represent the case of bubble crowding at low subcooling. In the present study this model is modified to consider the thickness of bubbly layer for wider range of subcooling.

3.1 The bubbly layer

It is observed in the experiment that the CHF increases significantly with the subcooling or mass flux increasing, while the wall superheat does not vary greatly. This suggests that the increase in critical heat flux with increase of subcooling or mass flux corresponds to a decrease in the critical thickness of bubbly layer. At very high flow and high subcooling condition the minimum thickness of bubbly layer is determined by the size of a bubble, while at low subcooling it could be larger due to bubble crowding. For the present experimental condition the following expression of the thickness of bubbly layer is attempted,

$$\delta = k_1 D_B (1 + k_2 e^{-k_3 \Pr Q}) \tag{3}$$

where factor k_1 , k_2 and k_3 are the constants, Pr is Prandtl number, Q is a parameter group (see

Eq.(13)). D_B is the bubble or vapor blanket equivalent diameter, evaluated by Staub correlation [13], as

$$D_{B} = \frac{32\sigma f(\beta)\rho_{L}}{fG^{2}} \tag{4}$$

where σ is the surface tension, ρ_L the liquid density, G the mass flux, $f(\beta)$ is a function with parameter of contact angle, and recommended value was $f(\beta) = 0.02 - 0.03$. In the present model it is used as

$$f(\beta) = 0.03$$
 for $p \le 10MPa$
 $f(\beta) = 0.03(1 - 0.055(p - 10))$ for $p > 10MPa$

where p is the pressure in MPa.

The f is friction factor, calculated by Colebrook-White equation combined with Levy's rough surface model [14], as

$$\frac{1}{\sqrt{f}} = 1.14 - 2.0 \log(\frac{\varepsilon}{D} + \frac{9.35}{\text{Re}\sqrt{f}})$$
 (5)

where D is the tube diameter, Re the Reynolds number, ε is the surface roughness, accounted by $\varepsilon = 0.75D_B$

The liquid core 3.2

The velocity distribution in the liquid core is represented by Karman's universal law, as in Celata's model [8],

$$U^{+} = y^{+} \qquad 0 \le Y^{+} < 5 \tag{6}$$

$$U^{+} = y^{+} \qquad 0 \le Y^{+} < 5 \qquad (6)$$

$$U^{+} = 5.0 \ln y^{+} - 3.05 \qquad 5 \le y^{+} < 30 \qquad (7)$$

$$U^{+} = 2.5 \ln y^{+} + 5.5$$
 $y^{+} \ge 30$ (8)

with

 $U^+ = \frac{U}{U}$

and

$$y^{+} = \frac{yU_{\tau}\rho_{L}}{\mu_{L}}$$

$$U_{\tau} = \left(\frac{\tau_{w}}{\rho_{L}}\right)^{0.5}$$

where U is the liquid velocity, y the distance from the wall, μ_L the liquid dynamic viscosity and ρ_L the liquid density, U_{τ} is the friction velocity, and τ_w is the wall shear stress, evaluated by

$$\tau_{w} = \frac{fG^{2}}{8\rho_{t}} \tag{9}$$

The temperature distribution in the liquid core is as follows [15],

$$T_0 - T = Q \operatorname{Pr} y^+$$
 $0 \le Y^+ < 5$ (10)

$$T_{0} - T = 5Q \left\{ \Pr + \ln \left[1 + \Pr(\frac{y^{+}}{5} - 1) \right] \right\}$$

$$T_{0} - T = 5Q \left[\Pr + \ln(1 + 5Pr) + 0.5 \ln(\frac{y^{+}}{30}) \right]$$

$$Q = \frac{q}{\rho_{L} C_{pL} U_{\tau}}$$

$$(13)$$

and

$$T_0 - T = 5Q \left[\Pr + \ln(1 + 5Pr) + 0.5 \ln(\frac{y^+}{30}) \right] \qquad y^+ \ge 30$$
 (12)

with

$$Q = \frac{q}{\rho_L C_{nl} U_{\tau}} \tag{13}$$

The equations (6 - 8 and 10-12) are assumed to be validate in the region of $\delta \le y \le R$, and the T_0 is a referent value to assure $T = T_s$ at $y = \delta$.

3.3 The calculation of critical heat flux

The local enthalpy, H, is calculated by

$$\dot{H} m = H_C (m - m_{B,g} - m_{B,L}) + H_g m_{B,g} + H_L m_{B,L}$$
(14)

where m is the total flow rate, $m_{B,g}$ and $m_{B,L}$ are the vapor and liquid flow rate in the bubbly layer, respectively, H_g and H_L are the vapor and liquid enthalpy, and H_C is the enthalpy of liquid core.

The m, $m_{B,g}$ and $m_{B,L}$ are evaluated as,

$$\dot{m} = \frac{\pi D^2}{4}G\tag{15}$$

$$\dot{m}_{B,g} = \pi (D - \delta) \delta \alpha_B \rho_g \overline{U_B} \tag{16}$$

and

$$\dot{m}_{B,L} = \pi (D - \delta) \delta (1 - \alpha_B) \rho_L \overline{U}_B \tag{17}$$

where $\alpha_{\scriptscriptstyle B}$ is the void fraction in the bubbly layer, and it is taken as $\alpha_{\scriptscriptstyle B}$ = 0.9, $\overline{U_{\scriptscriptstyle B}}$ is the average velocity of bubbly layer, estimated by

$$\overline{U_R} = 0.5U_{v=\delta}$$

The enthalpy of liquid core is evaluated at the average temperature from the edge of bubbly layer to the center of tube, T_C , calculated by

$$T_C = \frac{\int_{\delta}^{R} TU(R - y)dy}{\int_{\delta}^{R} U(R - y)dy}$$
 (18)

where R is the radius of tube, and δ , estimated by Eq.(3), is the distance from wall at which the temperature is equal to the saturation value.

The exit enthalpy, H is evaluated from the heat balance equation, as

$$H = H_i + \frac{4ql}{GD} \tag{19}$$

where H_i is the inlet enthalpy, and l is the heating length...

The calculation is started with a tested heat flux $(q < q_s)$, and the δ , $m_{B,g}$, $m_{B,L}$ and T_C are calculated by Eq. (3), (15), (16) and (17). Then, the H is calculated by Eq.(14), and is compared with that calculated by Eq.(19). The result of CHF is obtained through an iterative process.

To get the calculations better fit to the experimental data, the constants in Eq. (3) are as: $k_1 = 0.75$, $k_2 = 1000$, and $k_3 = 1.0$. At low subcooling q_{CHF} is close to q_s , and it is not sensitive to the δ . So in the analysis the maximum value of δ is simply set as 0.1D.

All the experimental data are calculated by the present model, as shown in Fig.9. The AVG is 0.1% and RMS is 4.9%.

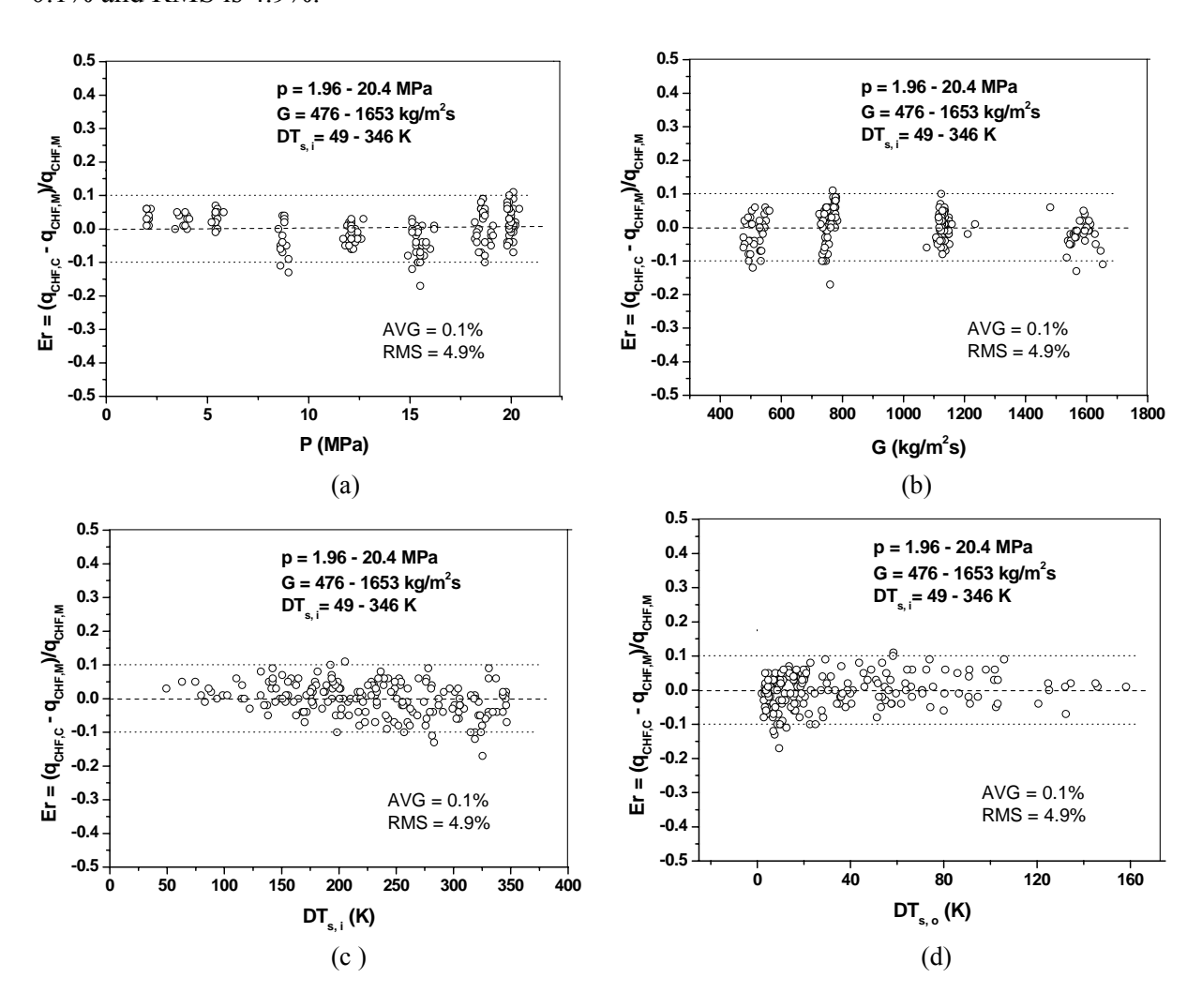


Figure 9 Comparison of the experimental results with the calculations of present model

4. Conclusions

An experiment of critical heat flux was conducted in an inconel tube with water flowing upward. The parametric trends of the critical heat flux were clarified, and a physical model was presented with assumption of critical thickness of the bubbly layer. Under these conditions the following conclusions are drawn:

- O The critical heat flux increases significantly with the increase of mass flux or inlet subcooling. At lower mass flux and lower subcooling the CHF is closely related with the inlet condition, characterizing the mechanism of total power dominant.
- O At lower pressure the effects of mass flux and subcooling on CHF are stronger than higher pressure. As pressure increases toward the critical point the critical heat flux tends to decrease, and it drops significantly at higher mass flux.
- O The material has a minor effect on the CHF by comparing the results of inconel tube and stainless-steel tube.

5. Acknowledgement

The present study was supported by National Basic Research Program of China (N0. 2007CB209800) and the Coordinated Research Project of International Atomic Energy Agency (IAEA Research contract No. 14469)

6. References

- [1] Thermohydraulic Relationships for Advanced Water Cooled Reactors, *IAEA-TECDOC* 1203 (2001)
- [2]. B.R. Vijayarangan, S. Jayanti, A.R. Balakrishan, "Studies on critical heat flux in flow boiling at near critical pressures", *Int. J. Heat and Mass Transfer*, V. 49, 259 268 (2006).
- [3] S. D. Hong, S. Y. Chun, S. Y. Kim and W. P. Beak, "Heat Transfer Characteristics of an Internally Heated Annulus Cooled with R-134a near the Critical Pressure", *J. Korean Nuclear Society*, V. 36, No. 5, 403-414 (2004).
- [4] S.Y. Chun, S.D.Hong, H. Kikura and M. Aritomi, "Critical Heat Flux in a Heater Rod Bundle Cooled by R-134a Fluid near the Critical Pressure", *Nucl. Science and Technology*, V. 44, No. 9, 1189 1198 (2007).
- [5] S. T. Yin, T. J. Lui, Y. D. Huang and R. M. Tain, "Measurements of Critical Heat Flux in Forced Flow at Pressures up to the Vicinity of the Critical Point of Water", *Proc. 1988 National Heat Transfer Conference in USA*, V. 1, 501-506 (1988).

- [6] Y. Chen, C. Yang, M. Zhao, K. Bi, K. Du and S. Zhang, "An Experimental Study of Critical Heat Flux in a Tube for Near-critical Pressures", Presented at ISSCWR-5, Canada, March, (2011)
- [7] L.S. Tong and Y.S. Tang, "Boiling Heat Transfer and Two-Phase Flow", Taylor & Francis, *ISBN 1-56032-485-6* (1997).
- [8] G. P. Celata, M. Cuma, A Mariani, M. Simosini and G Zummo, "Rationalization of Existing Mechanistic Models for the Prediction of Water Subcooled Flow Boiling Critical Heat Flux", Int. J. Heat and Mass Transfer 37, Suppl. 1, 347-360 (1994)
- [9]. J. Weisman and B. S. Pei, "Prediction of Critical Heat Flux in Flow Boiling at low qualities", Int. J. Heat Mass Transfer, 26, 1463 1477 (1983)
- [10] L. S. Tong, "Boundary Layer Analysis of the Flow Boiling Crisis", Int. J. Heat Mass Transfer, 11, 1208 1211 (1968)
- [11] Y. Katto, "A Prediction Model of Subcooled Water Flow Boiling CHF for Pressures in the region 0.1-20.0 MPa", Int. J. Heat ans Mass Transfer 35, 1115-1123 (1992).
- [12] C. H. Lee and I. Mudawar, "A Mechanistic Critical Heat Flux Model for Subcooled Flow Boiling Based on Local Bulk Flow Conditions", Int. J. Multiphase Flow, 14. 711-728 (1983).
- [13] F. W. Staub, "The Void Fraction in Subcooled Boiling Prediction of the initial Point of Net Vapor Generation, J. Heat Transfer, 90, 151-157 (1968)
- [14] S Levy, "Forced Convection Subcooled Boiling Prediction of Vapor Volumetric Fraction", Int. J. Heat Mass Transfer, 10, 951 965 (1967)
- [15] R. C. Martinelli, "Heat Transfer to Molter Metals", Trans. ASME 69, 947 951 (1947)